New Journal of Physics
The open access journal at the forefront of physics

Deutsche Physikalische Gesellschaft DPG
IOP Institute of Physics

Published in partnership with: Deutsche Physikalische Gesellschaft and the Institute of Physics

OPEN ACCESS

RECEIVED
8 April 2015

REVISED
25 July 2015

ACCEPTED FOR PUBLICATION
19 August 2015

PUBLISHED
16 September 2015

PAPER

Quantum state reconstruction on atom-chips

C Lovecchio[1], S Cherukattil[1], B Cilenti[2], I Herrera[1,3], F S Cataliotti[1,2,4], S Montangero[5], T Calarco[5] and F Caruso[1,2,4]

[1] LENS and Università di Firenze, Via Nello Carrara 1, 50019 Sesto Fiorentino, Italy
[2] Dipartimento di Fisica ed Astronomia, Università di Firenze, Via Sansone 1, 50019 Sesto Fiorentino, Italy
[3] Centre for Quantum and Optical Science, Swinburne University of Technology, Melbourne, Australia
[4] QSTAR, Largo Enrico Fermi 2, 50125 Firenze, Italy
[5] Institute for Complex Quantum Systems & Center for Integrated Quantum Science and Technology, University of Ulm, Albert-Einstein-Allee 11, D-89069 Ulm, Germany

E-mail: filippo.caruso@lens.unifi.it

Keywords: quantum information, atom-chips, quantum gases

Abstract

We realize on an atom-chip, a practical, experimentally undemanding, tomographic reconstruction algorithm relying on the time–resolved measurements of the atomic population distribution among atomic internal states. More specifically, we estimate both the state density matrix, as well as the dephasing noise present in our system, by assuming complete knowledge of the Hamiltonian evolution. The proposed scheme is based on routinely performed measurements and established experimental procedures, hence providing a simplified methodology for quantum technological applications.

1. Introduction

The use of measured data for the estimation of quantum states is crucial for the verification of the quality of any quantum device. To fully determine a quantum state, i.e. to perform a quantum state tomography, one needs to accumulate enough data to compute the expectation values of an informationally complete set of observables [1]. The availability of a complete set of measurements to be implemented by the experimenter is not straightforward and in general quantum state reconstruction is carried out by complicated set-ups that have to be robust against noise and decoherence sources, in order not to limit the accuracy of the reconstruction [2, 3].

The standard technique used in quantum optics for the full reconstruction of quantum states is coherent homodyne detection [4], which has recently been extended to ultracold atoms in [5]. Homodyne detection requires the use of a, not always available, local oscillator field that acts as a phase reference for the state under reconstruction [6]. A 'spin tomography' procedure which uses spin precession without the local oscillator is proposed in [7]. Other approaches were developed based either on the linear inversion of a set of observables [8], or on the maximum–likelihood estimation [9]. In both of these methods, to have a good estimation of the initial state one has to carefully design the measurements set in order to fulfil the informationally completeness that is required by the operator basis. A different approach is a least square minimization of a cost function, which permits the relaxation of some of the constraints on the data necessary to reconstruct the dynamics, and on the set of observables to measure [10]. For atomic internal states simpler interferometric techniques can be used to map the relative phases of internal components onto the level populations [11].

Cold atomic systems and degenerate quantum gases are unique tools for quantum simulations [6] and precision measurements of atom characteristics beyond the classical limit [12]. However, their applications outside of the laboratory depend critically on the simplification and downsizing of bulky cold-atom set-ups. Indeed, an interesting technological development is given by the possibility of integrating cold atoms with nanostructures [13]. An important invention in this direction is the realization of a Bose–Einstein Condensate (BEC) in microscopic magnetic traps based on the micro-electronics technology, yielding the so-called atom-chip [14, 15]. For example, experiments based on atom-chips have demonstrated nonlinear interferometers

with the sensitivity beyond the standard quantum limit [12], nonclassical interferometry with motional states [16], and quantum Zeno dynamics [17].

This work presents a practical, experimentally undemanding, tomography protocol that relies only on the time-resolved measurements of the atomic population distribution among atomic internal states. This protocol allows the reconstruction of a, not necessarily pure, state of a n-level quantum system, where the coherence elements are unknown and usually challenging to measure. The idea is simple: the state to be reconstructed evolves over time and the population distribution is measured at different times (see [8] for a similar data acquisition protocol); the same dynamics are numerically simulated starting from a randomly chosen initial state; we run an optimization protocol that minimizes the difference between the simulated and measured data in such a way that the optimal solution provides the tomographic reconstruction of the initial state—see also the reconstruction protocols in [9] and [10]. Our procedure is based on the complete knowledge of the system evolution. Note that, by applying the proposed scheme to a complete set of known states, one is, in principle, able to reconstruct the system dynamics, leading to a procedure similar to the quantum process tomography [18].

2. Experimental set-up

The experimental apparatus is based on a microscopic magnetic trap, or atom-chip [15, 19], where we bring an atomic sample of ^{87}Rb to quantum degeneracy through forced evaporative cooling. Most of the structures and wires necessary to the magnetic trapping, the forced evaporation and successive manipulation of the atoms are all embedded in the atom-chip, making this device versatile and experimentally easy to use [20]. Our BEC has typically 8 10^4 atoms in the low field seeking hyperfine state $|F = 2,\ m_F = 2\rangle$, at a critical temperature of 0.5 μK and is 300 μm away from the chip surface. The experiment described in this work is performed 0.7 ms after the BEC release from trap to guarantee a homogeneous magnetic bias field and strongly reduce the effects of atomic collisions. In this way the most relevant source of noise on the evolution turns out to be the instability of the environmental magnetic field.

We consider a n-level system represented by the five-fold $F = 2$ hyperfine ground level of ^{87}Rb. In the presence of a magnetic bias field the degeneracy between the magnetic sublevels is lifted according to the Breit—Rabi formula. Using two external Helmholtz coils, we arbitrarily set the magnetic field to 6.179 G[6]. To drive the atomic dynamics we apply a radio-frequency field (RF) oscillating at $\omega_{\rm RF} = 2\pi\ 4.323\ {\rm MHz}$[7] using a wire structure embedded in the chip. Due to the relative proximity between the BEC and the emitting wire with $\sim$10 mW of RF power we excite magnetic dipole transitions between the atomic levels at Rabi frequencies up to 200 kHz.

To record the number of atoms in each of the m_F states of the $F = 2$ hyperfine state we use a Stern–Gerlach method. After the state manipulation has been performed, in addition to the homogeneous bias field, we apply an inhomogeneous magnetic field along the quantization axis for 10 ms. This causes the different m_F states to spatially separate. After an expansion time of 23 ms a standard absorption imaging sequence is performed. The recorded atomic population in each m_F state is normalized to the total number of observed atoms.

It is important to stress that each measurement sequence completely destroys the system. This means that each sampling is associated to a different experimental cycle of production and manipulation of the BEC and we have to rest on the assumption that both the state preparation and the tomographic procedure always yield the same result. This assumption is a posteriori confirmed by the agreement between the prepared and reconstructed state. We sample every 5 oscillation of the RF field, corresponding to having a data point every $\sim$1.16 μs. We repeat 5 times each measurement to obtain the mean values of the relative atomic populations $p_{i,j} \equiv p_i(t_j)$ and standard deviations $\sigma_{i,j} \equiv \sigma_i(t_j)$ for each sublevel i. An example is represented in figure 1.

3. State reconstruction

The post-processing analysis is formulated in the following way: suppose that we want to estimate the initial quantum (not necessarily pure) state of a n-level system, described by the density operator $\rho_0 \equiv \rho(t = 0)$. To do that, we use the *a priori* known Hamiltonian operator $\hat{H}$ describing its dynamics and the measurements of the subsystem populations at different evolution times $p_i(t)$. In other words, we measure the observables $\hat{a}_i^\dagger \hat{a}_i$, hence obtaining the expectation values ${\rm Tr}[\rho(t)\hat{a}_i^\dagger \hat{a}_i] = p_i(t)$, where $\hat{a}_i$ and $\hat{a}_i^\dagger$ are, respectively, the

[6] The value of the field B is chosen around 6 G so that it is much larger than the magnetic noise fluctuations but, at the same time, the current used to produce it is not high enough to cause significant heating of the coils.

[7] The RF frequency $\nu_{\rm RF}$ is chosen to be 4.323 MHz in a way that the detuning with the energy differences between neighbouring levels $\omega_i - \omega_{i+1}$ at 6.179 Gauss is symmetric respect to the $m_f = 0$ level, for example $|\omega_1 - \omega_2 - 2\pi\nu_{\rm RF}| \approx |\omega_4 - \omega_5 - 2\pi\nu_{\rm RF}|$.

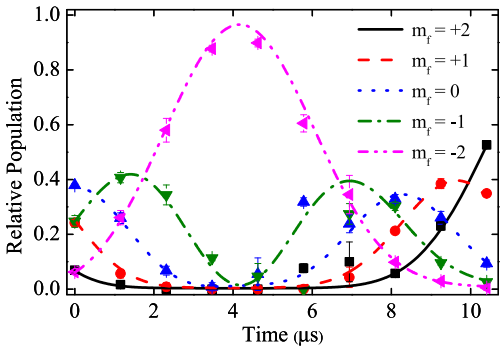

Figure 1. Time evolution of an arbitrary atomic state. An initial unknown state evolves under the effect of the Hamiltonian H and the five atomic populations (points) are recorded every 1.16 μs, i.e. every fifth oscillation of the RF field applied to the atomic sample. The superimposed line is the theoretical evolution with the estimated initial condition ρ_0 minimizing the deviation $\epsilon(\rho_0)$ between experimental and theoretical data.

annihilation and creation operators for each sublevel i, and $\rho(t)$ is the time-evolution of the unknown state ρ_0 that we want to estimate. In the case of fully coherent Hamiltonian evolution, one has $\rho(t) = \hat{U}(t)\rho_0\hat{U}(t)^\dagger$ with $\hat{U}(t) = \exp[-i\hat{H}t]$ being the unitary evolution operator. If the system is subjected to a noisy evolution instead , as it is the case in most experimental situation, one has $\rho(t) = \Phi_t(\rho_0)$ with Φ_t being the so-called quantum map or quantum channel or quantum operation mapping ρ_0 into $\rho(t)$ [21].

In our case the Hamiltonian, written in the rotating wave approximation, is

$$H = \hbar \begin{pmatrix} -\delta_2 & \Omega & 0 & 0 & 0 \\ \Omega & -\delta_1 & \sqrt{3/2}\,\Omega & 0 & 0 \\ 0 & \sqrt{3/2}\,\Omega & 0 & \sqrt{3/2}\,\Omega & 0 \\ 0 & 0 & \sqrt{3/2}\,\Omega & \delta_1 & \Omega \\ 0 & 0 & 0 & \Omega & \delta_2 \end{pmatrix}, \tag{1}$$

where the state basis is chosen to go from $m_F = +2$ to $m_F = -2$, the RF field Rabi frequency is $\Omega = 2\pi$ 60 kHz, the detunings δ_i are defined by $\delta_1 = 3$ kHz and $\delta_2 = 11$ kHz.

In order to include the unavoidable presence of dephasing noise, that mainly originated in our experiment from the presence of magnetic field fluctuations superimposed on the bias field, we add in our model a Lindblad super–operator term $\mathcal{L}$, acting on the density matrix ρ as $\mathcal{L}(\rho) = \sum_{j=1}^{5}\gamma[-\{\hat{a}_j^\dagger\hat{a}_j,\ \rho\} + 2\hat{a}_j^\dagger\hat{a}_j\ \rho\ \hat{a}_j^\dagger\hat{a}_j]$, which randomizes the phase of each sublevel j with a homogenous rate γ. We finally obtain the density matrix evolution as

$$\frac{\mathrm{d}}{\mathrm{d}t}\rho(t) = -\frac{\mathrm{i}}{\hbar}[H,\ \rho(t)] + \mathcal{L}(\rho(t)). \tag{2}$$

To summarize, in order to perform a tomographic reconstruction an initial unknown state evolves for a time T (tomography time) under the effect of the Hamiltonian H and the five atomic populations (points) are recorded every 1.16 μs. Note that this means that the number of measurements increases linearly with T.

To reconstruct the state one has n^2–1 unknown independent real parameters defining the $n \times n$ density matrix, with the constraint of leading to a physical state, i.e. a semi–definite positive, hermitian matrix ρ of unitary trace. This problem can be also formulated in the language of semi–definite programming [22]. It corresponds to finding the initial state ρ_0 minimizing the difference (e.g., mean squared error) between the measured populations $p_i(t_j)$ and the quantities $\mathrm{Tr}[\Phi_t(\rho_0)\hat{a}_i^\dagger\hat{a}_i]$ for each observed time step t_j, hence $\min_{\rho_0}\sum_{i,j}||\mathrm{Tr}[\Phi_{t_j}(\rho_0)\hat{a}_i^\dagger\hat{a}_i] - p_i(t_j)||$ with $\Phi_t(\rho_0)$ mapping ρ_0 into $\rho(t)$ being the solution of the master equation in (2), and $||\cdot||$ being any mathematical norm. Here, we have implemented the minimization algorithm using the Subplex variant of the Nelder–Mead method [23]. In particular, to take into account also the experimental uncertainties, we minimize, with respect to ρ_0, the following weighted mean squared deviation function

$$\epsilon(\rho_0) = \frac{1}{5}\sum_i\sqrt{\left(\sum_j\omega_{i,j}\left|\bar{p}_{i,j}(\rho_0) - p_{i,j}\right|^2\right)/\sum_j\omega_{i,j}}, \tag{3}$$

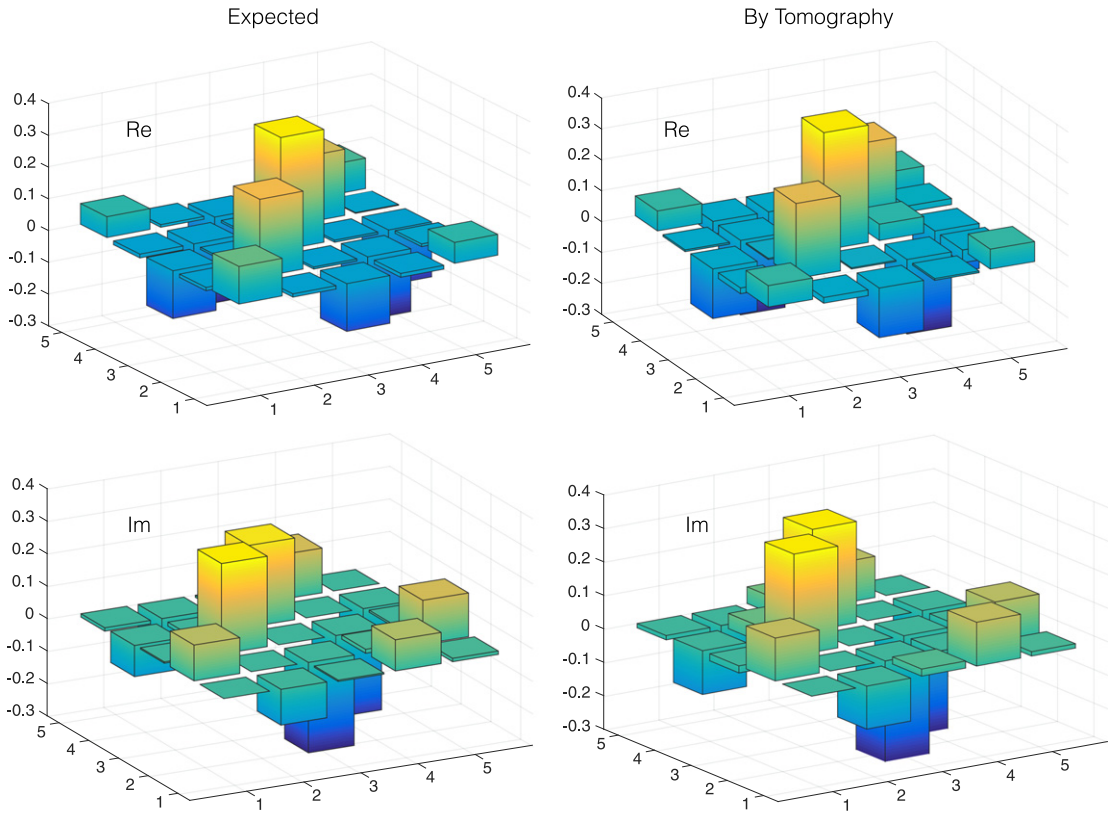

Figure 2. Pictorial representation of the theoretically expected density matrix $\rho_{\rm in}$ (left) and the reconstructed one ρ_0 (right), with the real (upper) and the imaginary (lower) components. The Uhlmann fidelity $\mathcal{F}(\rho_0,\,\rho_{\rm in})$ between ρ_0 and $\rho_{\rm in}$ is $\mathcal{F}=0.98$.

where $\bar{p}_{i,j}(\rho_0)={\rm Tr}[\Phi_{t_j}(\rho_0)\hat{a}_i^\dagger\hat{a}_i]$ and $\omega_{i,j}\equiv 1/\sigma_{i,j}^2$. The constraints of Hermitianicity and positiveness of the output density matrix are inserted in the minimization algorithm as a penalty function which automatically excludes the non–physical results.

4. Results

To test our scheme, we have prepared, by applying known Hamiltonian evolutions, a set of states to be reconstructed. Since the preparation can be affected by experimental errors, the real states can be different from the expected. From numerical simulations based on the knowledge of the preparation Hamiltonians, we compute the expected theoretical density matrices $\rho_{\rm in}$. For example, in figure 1 we reconstruct a state that is obtained by applying a $\pi/2$ pulse[8] to the $|F=2,\,m_F=2\rangle$ state. We report the experimentally recorded population evolutions in a 16 μs-long time window. We then compare these results with the theoretical evolutions of the diagonal elements (i.e. populations) of the reconstructed state ρ_0. For this reconstruction, based on 16 averaged observations of the five-level populations, the computed deviation is $\epsilon\,(\rho_0)\sim 2\times 10^{-6}$, corresponding to an Uhlmann fidelity [24] of $\mathcal{F}(\rho_0,\,\rho_{\rm in})=0.98$ between the reconstructed density matrix ρ_0 and the expected theoretical one $\rho_{\rm in}$, that are pictorially represented in figure 2. Let us point out that no a priori knowledge of the initial state has been used for the tomographic reconstruction. However, this information has been exploited to calculate the Uhlmann fidelity.

Moreover, we have faithfully reconstructed, with deviations below 3×10^{-6}, other states prepared by using the Hamiltonian in equation (1) and randomly varying over time the detunings δ_1 and δ_2. These low deviations correspond to fidelities higher than 0.95.

To check the reconstruction error convergence, with respect to the number of collected data, we applied the optimization algorithm to the population distributions in different time windows T, and computed the quantity $1-\mathcal{F}(\rho_0,\,\rho_{\rm in})$ in each case. The results in figure 3 show that when T is comparable with the system natural evolution timescale ($T\sim 2\pi/\Omega$), the reconstruction accuracy is already satisfactory, with the error quickly saturating to its minimum value.

[8] A $\pi/2$ pulse corresponds to the application of the Hamiltonian in equation (1) for one fourth of a period, i.e. $\pi/(2\,\Omega)$, that is about 4 μs in our case.

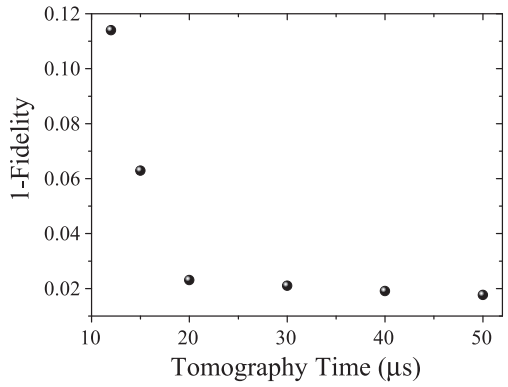

Figure 3. Behaviour of $1 - \mathcal{F}(\rho_0, \rho_{in})$ versus the tomography time (used to minimize the deviation $\epsilon(\rho_0)$), where $\mathcal{F}(\rho_0, \rho_{in})$ is the Uhlmann fidelity between ρ_0 and ρ_{in}, ρ_0 is the state reconstructed from the experimental data, and ρ_{in} the expected one.

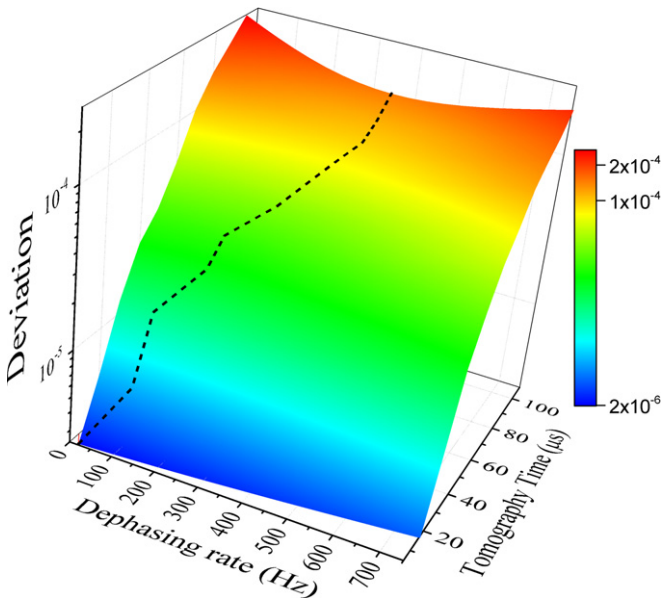

Figure 4. Deviation $\epsilon(\rho_0)$ as a function of the tomography time T_i (reconstruction window $[0, T_i]$) and the dephasing rate γ. For clarity the value of the deviation ϵ is color coded according to the legend on the right. For any given value of the tomography time T_i it is possible to minimize the deviation ϵ (dashed line) to obtain the value γ_{opt} of the dephasing rate.

Furthermore, this technique can be also exploited to get further information on the system evolution, e.g. to estimate the amount of dephasing noise in the system dynamics resulting from its coupling to the external environment. More specifically, we have reconstructed the initial density matrix by measuring the population evolution within different time windows $[0, T_i]$, with $T_i \in [10, 100]$ μs, but neglecting the presence of dephasing, i.e. $\gamma = 0$. Then, for any reconstruction, we have found the value of dephasing rate $\gamma_{opt} \in [0, \quad 750]$ Hz, minimizing the deviation ϵ between the theoretical and experimental data–see figure 4. Note that, the same optimal results have been obtained when both the state and the dephasing rate were optimized at the same time, with the scheme above providing however a faster optimization procedure. It turns out that the optimal dephasing rate increases with the tomography time T_i, hence selecting the noise spectrum components larger than $1/T_i$, as expected. In other terms, another possible application of our procedure is to quantify the rate of the dephasing noise affecting the system evolution by means of the optimized reconstruction procedure, hence indirectly extracting information on the strength of the coupling between the system and the external environment. We expect this to allow one to the characterizate the type of external noise, with the additional possibility of identifying the presence of temporal noise correlations.

5. Conclusions

To summarize, we have experimentally demonstrated a tomographic reconstruction algorithm that relies on data collected during the evolution of an unknown quantum state, assuming a complete knowledge of the system Hamiltonian. The advantages of this protocol are the simplicity of the post-processing procedure and the use of a quite conventional absorption imaging technique. Furthermore, we have shown the convergence of the protocol even when using a small amount of collected data, compared to standard tomographic technique. Finally, we have also estimated the rate of the dephasing noise present in our system dynamics by repeating this procedure for longer tomography time windows and minimizing the reconstruction deviation.

Moving another step further, a promising application may be represented by the possibility of characterizing the noise itself, for instance its spatial and temporal correlations, by investigating the behaviour of the state reconstruction error in terms of different noise models. The proposed scheme therefore realizes quantum state tomography, but could readily be modified to perform quantum process tomography by assuming complete knowledge of the input states, hence providing a very feasible and useful tool for several quantum technological applications.

Acknowledgments

This work was supported by the Seventh Framework Programme for Research of the European Commission, under FET-Open grant MALICIA, QIBEC, SIQS, by MIUR via PRIN 2010LLKJBX, and by DFG via SFB/TRR21. The work of F C has been supported by EU FP7 Marie Curie Programme (Career Integration Grant No. 293449) and by MIUR–FIRB grant (Project No. RBFR10M3SB). We thank M Inguscio for fruitful discussions and continuous support.

References

[1] Paris M and Rehácek J (ed) 2004 *Quantum State Estimation* (Berlin: Springer)
[2] Lvovsky A I and Raymer M G 2009 *Mod. Phys. Rev.* **81** 299
[3] Hansen H, Aichele T, Hettich C, Lodahl P, Lvovsky A I, Mlynek J and Schiller S 2001 *Opt. Lett.* **26** 1714
[4] Walls D and Milburn G 2008 *Quantum Optics* (Berlin: Springer)
[5] Gross C *et al* 2011 *Nature* **480** 219
[6] Bloch I, Dalibard J and Zwerger W 2008 *Mod. Phys. Rev.* **80** 885
[7] D'Ariano G M, Maccone L and Paini M 2003 *J. Opt. B: Quantum Semiclass. Opt* **5** 77
[8] Klose G, Smith G and Jessen P S 2001 *Phys. Rev. Lett.* **86** 4721
[9] Silberfarb A, Jessen P S and Deutsch I H 2005 *Phys. Rev. Lett.* **95** 030402
[10] Smith A, Riofrio C A, Anderson B E, Sosa-Martinez H, Deutsch I H and Jessen P S 2013 *Phys. Rev.* A **87** 030102(R)
[11] Cronin A D, Schmiedmayer J and Pritchard D 2009 *Mod. Phys. Rev.* **81** 1051
[12] Gross C, Zibold T, Nicklas E, Estève J and Oberthaler M K 2010 *Nature* **464** 1165
[13] Gierling M *et al* 2011 *Nat. Nanotechnol.* J **6** 446
[14] Hänsel W, Reichel J, Hommelhoff P and Hänsch T W 2001 *Phys. Rev. Lett.* **86** 608
[15] Folman R, Krüger R, Schmiedmayer J, Denschlag J and Henkel C 2002 *Adv. Atom. Mol. Opt. Phys.* **48** 263
[16] van Frank S *et al* 2014 *Nat. Commun.* **5** 4009
[17] Schäfer F, Herrera I, Cherukattil S, Lovecchio C, Cataliotti F S, Caruso F and Smerzi A 2014 *Nat. Commun.* **5** 3194
[18] D'Ariano G M and Lo Presti P 2004 *8 Characterization of Quantum Devices Quantum State Estimation* ed M Paris and J Rehácek (Berlin: Springer) p 297
[19] Förtagh J and Zimmermann C 2007 *Mod. Phys. Rev.* **79** 235
[20] Petrovic J, Herrera I, Lombardi P, Schäfer F and Cataliotti F S 2013 *New. J. Phys.* **15** 043002
[21] Caruso F, Giovannetti V, Lupo C and Mancini S 2014 *Mod. Phys. Rev.* **86** 1203
[22] Wunderlich H, Virmani S and Plenio M B 2010 *New J. Phys.* **12** 083026
[23] Rowan T 1990 Functional stability analysis of numerical algorithms *Phd Thesis* University of Texas, Austin
[24] Nielsen M A and Chuang I L 2000 *Quantum Computation and Quantum Information* (Cambridge: Cambridge University Press)